THE JOURNAL OF BIOLOGICAL CHEMISTRY
Vol. 274, No. 38, Issue of September 17, pp. 27119–27127, 1999

Printed in U.S.A.

Quantitative Relationship among Integrin-Ligand Binding, Adhesion, and Signaling via Focal Adhesion Kinase and Extracellular Signal-regulated Kinase 2*

(Received for publication, May 5, 1999, and in revised form, July 1, 1999)

Anand R. Asthagiri‡§, Celeste M. Nelson‡¶, Alan F. Horwitz‖, and Douglas A. Lauffenburger‡**

From the ‡Department of Chemical Engineering, Division of Bioengineering and Environmental Health, and Center for Cancer Research, Massachusetts Institute of Technology, Cambridge, Massachusetts 02139 and the ‖Department of Cell Biology, University of Virginia, Charlottesville, Virginia 22908

Because integrin-mediated signals are transferred through a physical architecture and synergistic biochemical network whose properties are not well defined, quantitative relationships between extracellular integrin-ligand binding events and key intracellular responses are poorly understood. We begin to address this by quantifying integrin-mediated FAK and ERK2 responses in CHO cells for varied $\alpha_5\beta_1$ expression level and substratum fibronectin density. Plating cells on fibronectin-coated surfaces initiated a transient, biphasic ERK2 response, the magnitude and kinetics of which depended on integrin-ligand binding properties. Whereas ERK2 activity initially increased with a rate proportional to integrin-ligand bond number for low fibronectin density, the desensitization rate was independent of integrin and fibronectin amount but proportional to the ERK2 activity level with an exponential decay constant of 0.3 (± 0.08) min^{-1}. Unlike the ERK2 activation time course, FAK phosphorylation followed a superficially disparate time course. However, analysis of the early kinetics of the two signals revealed them to be correlated. The initial rates of FAK and ERK2 signal generation exhibited similar dependence on fibronectin surface density, with both rates monotonically increasing with fibronectin amount until saturating at high fibronectin density. Because of this similar initial rate dependence on integrin-ligand bond formation, the disparity in their time courses is attributed to differences in feedback regulation of these signals. Whereas FAK phosphorylation increased to a steady-state level as new integrin-ligand bond formation continued during cell spreading, ERK2 activity was decoupled from the integrin-ligand stimulus and decayed back to a basal level. Accordingly, we propose different functional metrics for representing these two disparate dynamic signals: the steady-state tyrosine phosphorylation level for FAK and the integral of the pulse response for ERK2. These measures of FAK and ERK2 activity were found to correlate with short term cell-substratum adhesivity, indicating that signaling via FAK and ERK2 is proportional to the number of integrin-fibronectin bonds.

Integrins are adhesion receptors that not only provide the mechanical link between the cell and the extracellular matrix (ECM)[1] that is essential for adhesion, spreading, and migration (1, 2), but also generate intracellular signals that affect multiple cell functions (3–5). Altered cell behavior due to aberrant regulation of these signals results in pathologies, such as cancer, in which loss of integrin signaling-based control of cell cycle progression leads to anchorage-independent cell growth and tumor formation (6). Because of these significant and wide-ranging regulatory roles, modulating integrin-mediated signals may provide powerful targets for disease therapy. Furthermore, since integrins interface cells to biomaterials, biomimetic surfaces may be designed to instigate appropriate integrin-mediated signals to elicit desired cell behavior on these surfaces. However, several issues must be addressed before rational design can be undertaken for controlled manipulation of these signals for such applications.

The first such issue derives from the complexity of the multiple pathways and numerous signaling molecules that connect the extracellular stimulus to intracellular signals. These signals emanate from focal adhesion complexes, which are formed upon aggregation of ligand-bound integrins and are composed of intracellular and transmembrane proteins held together by noncovalent intermolecular associations (7). In addition to the poorly characterized physical architecture of these complexes and the mechanisms of its assembly, biophysical phenomena, such as diffusion to and from the plasma membrane and molecular crowding in multiprotein complexes, could inhibit the progress of these pathways (8). Furthermore, the downstream non-membrane-associated signaling events are highly interconnected, and clarification of their operational synergy is only beginning to emerge. Because of the complexity within each hierarchy of events leading to integrin signals (9), it is not intuitively apparent how the extracellular ligand binding event quantitatively relates to intracellular signaling responses. This fundamental relationship is essential to a better understanding of the cumulative performance of the synergistic mechanisms underlying integrin-mediated signaling. In this study, we begin to address this by quantifying FAK phosphorylation and ERK2 activation in response to manipulating $\alpha_5\beta_1$ integrin interaction with its ligand, Fn.

The focus on FAK and ERK2 is based not only on their significance in regulating multiple cell functions (10–14) but also on the controversy surrounding the role of FAK as an upstream component in integrin-mediated ERK2 activation

* This work was funded by NIGMS, National Institutes of Health Grants 53905 (to D. A. L.) and 23244 (to A. F. H.). The costs of publication of this article were defrayed in part by the payment of page charges. This article must therefore be hereby marked "*advertisement*" in accordance with 18 U.S.C. Section 1734 solely to indicate this fact.

§ Partially supported by the National Institutes of Health Biotechnology Training Grant at the Massachusetts Institute of Technology and by a grant from Johnson & Johnson Professional, Inc.

¶ Present address: Department of Biomedical Engineering, The Johns Hopkins University, Baltimore, MD 21205.

** To whom correspondence should be addressed. Tel.: 617-252-1629; Fax: 617-258-0204; E-mail: lauffen@mit.edu.

[1] The abbreviations used are: ECM, extracellular matrix; FAK, focal adhesion kinase; ERK, extracellular signal-regulated kinase; CHO, Chinese hamster ovary; MAPK, mitogen-activated protein kinase; PBS, phosphate-buffered saline; MEK, MAP kinase kinase; PL, poly-L-lysine; Fn, fibronectin.

(15–19). Therefore, in addition to relating integrin-ligand binding to these signals in a dose-response signaling study, we compare the dynamic portions of FAK and ERK2 signals to determine whether the kinetics are reflective of FAK phosphorylation being upstream of ERK2 activation. Furthermore, by undertaking this kinetic analysis, we aim to develop a rigorous methodology for quantitatively comparing signals that are often-observed to be dynamic and diverse. For example, MAPK activity was measured to be a transient response spanning 60 min in Swiss 3T3 fibroblasts but was long-lived in NIH3T3 cells, maintaining a nonbasal steady-state level for up to 180 min (20, 21). Within the same cell system, altering the form of stimulation produced a transient *versus* sustained MAPK response (21). In addition, even for a fixed stimulation in the same cell type, FAK phosphorylation and ERK2 activity followed disparate time courses (22). Given this diversity in signaling responses, it is essential to determine what properties of these signals can be used to ascertain latent correlations and to gain insight into the regulatory mechanisms, both positive and negative, affecting these signals.

In our system, analysis of the dynamics of the ERK2 and FAK response revealed that (*a*) FAK and ERK2 activation by integrin/Fn binding may involve pathways having some parallel character; (*b*) the initial rate of signaling via ERK2 is proportional to integrin-ligand bond number; (*c*) ERK2 deactivation is driven by feedback mechanisms operating at a rate determined by the amount of active ERK2 and with a rate constant independent of integrin/Fn binding; (*d*) despite the superficial disparity in the FAK and ERK2 time courses, the initial rates of both responses have a similar dependence on Fn density; and (*e*) the disparity stems from different desensitization mechanisms regulating FAK and ERK2. Finally, metrics proposed for representing these dynamic signals were shown to quantitatively correlate to their common stimulus of integrin/ligand binding and cell adhesion.

MATERIALS AND METHODS

Antibodies and Reagents—Human plasma Fn and PL was obtained from Sigma. The human α5 cDNA (23) and the 6F4 anti-human α5 antibody were gifts from Dr. Louis Reichardt (University of California, San Fransisco, CA) and Dr. Ralph Isberg (Tufts University), respectively. The sc-154 anti-ERK2 antibody was purchased from Santa Cruz Biotechnology. The E10 monoclonal antibody (New England Biolabs) was used to detect phospho-p44/42 MAP kinase, and total ERK1/2 amounts were probed with the pan-ERK antibody (Transduction Laboratories). The sc-558 anti-FAK antibody (Santa Cruz Biotech) and the 2A7 monoclonal anti-FAK antibody (Upstate Biotechnology) were used for Western blotting and immunoprecipitation, respectively.

Cell Culture—CHO-B2 cells transfected with human α5 integrin subunit as described previously (24) were maintained under selection with 500 μg/ml Geneticin (Life Technologies, Inc.) in Dulbecco's modified Eagle's medium supplemented with 10% (v/v) fetal bovine serum, 4 mM L-glutamine, 1 mM sodium pyruvate, and 1% (v/v) 100× nonessential amino acids. CHO cells expressing human α5 integrin were divided into subpopulations based on their $\alpha_5\beta_1$ integrin expression levels using fluorescence-activated cell sorting (24). Sorted cells were grown and frozen for later use.

Protein-coating Surfaces and Quantification of Fn Coating Density—Fn or PL diluted in PBS was incubated overnight at 4°C in Nunc tissue culture-treated plastic dishes. The dishes were then washed twice with cold PBS and blocked for 1 h at 37 °C with 2 mg/ml sterile-filtered, heat-inactivated (70°C, 1 h) bovine serum albumin in PBS. Prior to use, the dishes were washed twice with warm PBS.

Fn coating density was quantified using Fn labeled with ^{125}I using the manufacturer's protocol for Iodobeads (Pierce). Radioisotope-labeled Fn was coated onto Nunc tissue culture plastic as described above, including the bovine serum albumin block and the final two warm PBS washes. The Fn remaining on the dish was removed using a series of incubations and washes with 1 M NaOH and 10× trypsin (Sigma). Fluid from each wash and strip incubation was collected, and the amount of radioactivity was measured with a gamma counter (Packard).

Serum Starvation and Stimulation on Protein-coated Surface—Cells were serum-starved on 100-mm tissue culture dishes for 18 h in serum-free media containing 25 mM Hepes-based Dulbecco's modified Eagle's medium, 500 μg/ml Geneticin, 4 mM L-glutamine, 1 mM sodium pyruvate, 1% (v/v) 100× nonessential amino acids, and 2 mg/ml bovine serum albumin. Cells were suspended using versene (Life Technologies, Inc.) and resuspended in serum-free medium to a concentration of 5×10^5 cells/ml. They were maintained in suspension for 1 h to bring adhesion-related signals to a basal level.

Serum-starved cells were plated onto Fn-coated 60-mm dishes and were incubated at 37°C. At desired times, they were washed once with cold PBS and lysed by adding cold lysis buffer containing 50 mM Tris (pH 7.5), 150 mM sodium chloride, 50 mM β-glycerophosphate (pH 7.3), 10 mM sodium pyrophosphate, 30 mM sodium fluoride, 1% Triton X-100, 1 mM benzamidine, 2 mM EGTA, 100 μM sodium orthovanadate, 1 mM dithiothreitol, 10 μg/ml aprotinin, 10 μg/ml, 1 μg/ml pepstatin, and 1 mM PMSF. The lysis buffer for FAK studies was more stringent, containing 0.5% Nonidet P-40 and 0.25% sodium deoxycholate. Cells were scraped into the buffer and allowed to lyse for approximately 15 min. Lysates were centrifuged at 14,000 rpm for 15 min, and the supernatant was collected. Micro-BCA protein determination (Pierce) was used to determine total protein concentration.

ERK2 Kinase Activity and Phosphorylation Assay—ERK2 kinase activity was measured using a sensitive *in vitro* assay performed in a 96-well format as described previously (25). Briefly, anti-ERK2 antibody was coated on the surface of Reacti-Bind™ protein A-coated wells (Pierce) by incubating wells with 10 μg/ml sc-154 antibody overnight at 4°C. After the wells were washed, 25 μg of cell lysate was incubated for 3 h at 4°C. To measure background, an extra well was incubated with just lysis buffer and was carried through the assay in the same manner as other samples. After washing, each well was resuspended in buffer containing 20 mM Tris (pH 7.5), 15 mM magnesium chloride, 5 mM β-glycerophosphate (pH 7.3), 1 mM EGTA, 0.2 mM sodium orthovanadate, and 0.2 mM dithiothreitol. To each well, 40 μg of myelin basic protein (Sigma) was added. The *in vitro* reaction was initiated by adding 25 μM ATP (1 μCi of [γ-^{32}P]ATP). After 30 min of agitation at 37 °C, reactions were quenched with 75 mM phosphoric acid. The quenched reaction contents were filtered through a 96-well phosphocellulose filter plate using the Millipore Multiscreen® system (Millipore). After washes, ^{32}P label on each filter paper was quantified using CytoScint™ (ICN Biomedicals) scintillation fluid and RackBeta (Wallac) scintillation counter. ^{32}P measurements were adjusted by subtracting the radioactivity associated with the background sample.

For determining dually phosphorylated ERK1/2 levels, whole cell lysates (15 μg) were resolved in 10% SDS-polyacrylamide gel electrophoresis and blotted onto PVDF membrane. Blots were probed using 1:5000 dilution of E10 anti-phospho-ERK1/2 antibody. After analyzing the blot, it was stripped and reprobed for total ERK1/2 levels using 1:5000 dilution of pan-ERK antibody.

FAK Phosphorylation Assay—FAK was immunoprecipitated from 100 μg of cell lysate using ~2 μg of 2A7 anti-FAK antibody coated on anti-mouse IgG beads (Sigma). After four washes, 30 μl of 1× SDS sample buffer was added to the immunoprecipitate, and the sample was boiled for 5 min. The sample was resolved under 7.5% SDS-polyacrylamide gel electrophoresis and transferred onto nitrocellulose membrane. Blots were probed for phosphotyrosine using 1:2500 dilution of RC20H and the SuperSignal® Ultra substrate (Pierce). After analyzing the blot, it was stripped by incubating in 62.5 mM Tris-Cl, pH 6.8, 2% SDS, 100 mM β-mercaptoethanol at 60 °C for 30 min and probed for total FAK using 1:100 dilution of sc-558 antibody. Bands were visualized with the Molecular Imager® system (Bio-Rad), and further analysis and quantification were performed with the Multi-Analyst® software (Bio-Rad). FAK phosphorylation levels were normalized to the amount of total FAK recovered from each immunoprecipitate.

Centrifuge Adhesion Assay—Nunc tissue culture-treated 96-well plates were coated with varying amounts of Fn (5 wells for each Fn amount). A set of negative-control wells with no Fn was also prepared. A positive-control plate coated with 20 μg/ml PL was prepared to support attachment of all plated cells.

Serum-starved cells were plated in these wells and allowed to adhere at 37 °C for 10 min. During the next 10 min, cells continued to adhere to the surface while the plate was being prepared for centrifugation. In total, cells were given 20 min to form their attachments to the surface. The wells were prepared for centrifugation by filling them completely with serum-free medium and sealing them. The plates containing both the Fn-coated and negative-control wells were inverted and centrifuged for 10 min at room temperature. The positive-control plate was inverted but not centrifuged.

After centrifugation, the seals were removed, and the contents of all

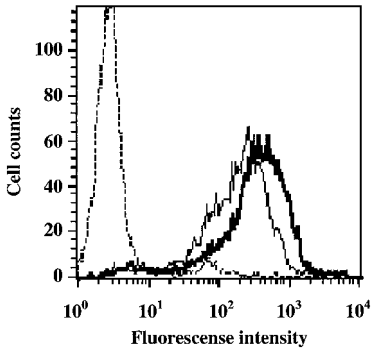

FIG. 1. **CHO cells were sorted into 1× and 1.7× relative α5 integrin subunit expression levels.** CHO-B2 cells were transfected with human α5 cDNA and were sorted into subpopulations based on their α5 expression. These sorted cells were grown and frozen for storage. After a passaging scheme and serum-starvation protocol that was also used for each signaling and adhesion experiment, the relative α5 expression levels were checked by flow cytometry. A control sample (*broken line*) with just secondary antibody treatment was used to determine background fluorescence. The relative $\alpha_5\beta_1$ integrin expression levels were determined to be 1× (*thin solid line*) and 1.7× (*heavy solid line*).

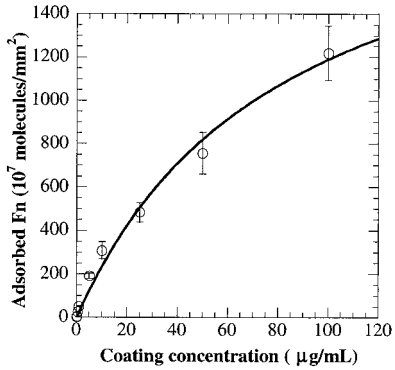

FIG. 2. **Fibronectin adsorption was a nonlinear, monotonically increasing function of coating concentration.** After coating tissue culture dishes with radioisotope-labeled fibronectin in a manner consistent with surface preparation for signaling and adhesion experiments, the amount of fibronectin adsorbed onto the surface was quantified. The adsorption data was fit to a Langmuir single-site model described by $A = A_{max} \cdot C_c/(K_a + C_c)$, where A is the amount of adsorbed fibronectin, C_c is the coating concentration, A_{max} is the surface density at saturation, and K_a is the coating concentration required to achieve half-maximal adsorption ($r^2 = 0.99$). *Error bars* represent the S.D. computed from three independent experiments.

wells were aspirated. While the plates were kept on ice, cells were lysed for 5 min in 20 μl of cold 0.5% Triton X-100 in PBS. In the meantime, lactate dehydrogenase reagent (Sigma) was prepared by mixing 10 parts reagent A to 0.4 parts reagent B. Lactate dehydrogenase reagent was added to each well and the mixture was transferred to an UV Spectra plate (Corning Costar). The absorption at 340 nm (A_{340}) was read for 3 min, every 12 s on a Spectramax (Molecular Dynamics). The A_{340} readings for the negative-control wells were treated as background and were subtracted from the other measurements. The rate of A_{340} decrease is proportional to the number of cells in each well. The fraction of cells detached due to centrifugation was calculated as 1 minus the ratio of the rate of A_{340} decrease in the wells that were centrifuged to the rate of A340 decrease in the positive-control well. From this data, the mean detachment force required to detach 50% of the cells was calculated.

Adhesion Wash Assay—Serum-starved CHO cells were plated in microtiter wells in serum-free medium with 1 mM RGD, 1 mM RGE, or no peptide. After allowing cells to adhere and spread for 1 h, a picture was taken using a Nikon camera attached to a phase-contrast microscope. Then, the plate was pulsed four times at 800 rpm on a plate shaker to dislodge weakly adhered cells. After a single wash with PBS, cell number was quantified using the lactate dehydrogenase assay as described above.

RESULTS

Modulation of $\alpha_5\beta_1$ Integrin and Fn Levels—To quantitatively relate integrin-ligand binding to integrin-mediated signaling, $\alpha_5\beta_1$ integrin-Fn binding was manipulated by altering both $\alpha_5\beta_1$ integrin expression level and Fn coating density. Two CHO cell populations with relative mean $\alpha_5\beta_1$ integrin expression levels of 1 and 1.7 were obtained by fluorescence-activated cell sorting of a CHO-B2 cell line that was transfected with cDNA encoding the human α5 integrin subunit (Fig. 1).

The amount of adsorbed Fn was varied by incubating tissue culture plastic with solutions of different fibronectin concentration. Radioisotope-labeled Fn was used to directly measure the amount of Fn coated on the surface (Fig. 2). The adsorption isotherm fit a curve described by the Langmuir model for single species adsorption to a single site on the substratum, and maximum coverage was predicted to be 2.2 (± 0.3) × 10^{10} molecules/mm^2 or 16 (± 2.2) ng/mm^2, assuming a molecular mass of 450 kDa. This value is in agreement with the theoretically predicted saturation density of 3.2 × 10^{10} molecules/mm^2 from a close-packing model that assumes cylindrical dimensions of length 60 nm and base diameter 6 nm for the Fn molecule (26). Half-maximal adsorption occurred at a coating concentration of 83 (± 20) μg/ml or 180 (± 43) nM. We used coating concentrations in the range of 0.1–10 μg/ml yielding surface Fn densities of 5.3–310 × 10^7 molecules/mm^2. Adsorption was not a linear function of coating concentration as a 100-fold increase in coating concentration yielded only a 60-fold increase in surface density, indicating the importance of directly measuring levels of adsorbed Fn.

Magnitude and Kinetics of ERK2 Response Depend on Integrin-Ligand Binding Properties—Because our focus was to quantify signaling induced specifically by $\alpha_5\beta_1$ integrin-Fn interactions, cells were stimulated by plating on Fn-coated surfaces under serum-free conditions to avoid additive signaling effects from growth factors and other ECM proteins present in serum. Signaling synergy between growth factor receptors and integrins is well documented and would thwart our ability to make clear conclusions about signaling responses caused solely by the binding of $\alpha_5\beta_1$ integrin to Fn (27–30).

In order to study the full effect of changing integrin-ligand binding properties, the entire time course of the ERK2 signal was measured at each condition. The challenge of such a study is that the number of parameters was enlarged to include not only two $\alpha_5\beta_1$ integrin expression levels and five Fn amounts, but also several time points. In total, this involved ERK2 activity measurement of ~60 samples per trial. To handle such a large quantity of samples, we developed and utilized a modified microtiter ERK2 activity assay that allowed for convenient and concurrent processing of multiple samples (25). Using this method, the measured time course of ERK2 activity revealed quantitative variations in response to changes in integrin-ligand binding properties (Fig. 3, *A* and *B*). This observed ERK2 response was initiated specifically by cell adhesion to Fn, as plating cells on PL failed to induce a response (Fig. 3*C*).

For each integrin expression level, a change in Fn density altered both the magnitude and kinetics of the ERK2 response. When Fn amount was increased, ERK2 activity reached a higher peak level within a shorter time. For example, for the 1× $\alpha_5\beta_1$ expression level, an increase in Fn coating density from 5 × 10^7/mm^2 to 310 × 10^7/mm^2 increased the peak activity level approximately 5-fold and reduced the time required to reach this peak from ~10 to ~5 min. The initial rate of ERK2 activation affects both the magnitude of the peak and the time required to reach this peak. We calculated this initial ERK2 activation rate as the slope of the time course between the 0- and 5-min time points. Higher initial rates of ERK2 activation

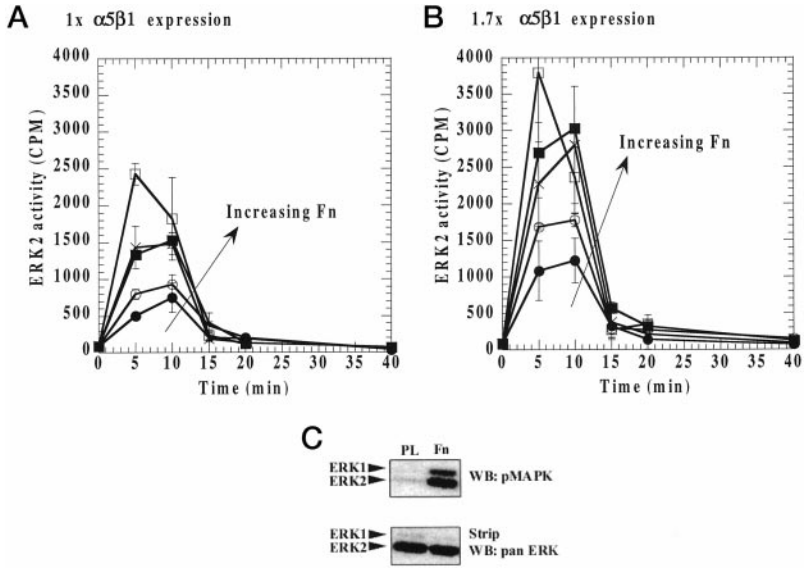

FIG. 3. **Both the magnitude and the kinetics of the ERK2 time course depends on $\alpha_5\beta_1$ integrin expression level and fibronectin density.** ERK2 activity was measured in response to plating serum-starved CHO cells with relative $\alpha_5\beta_1$ integrin expression levels of 1× (*A*) and 1.7× (*B*) on surfaces with fibronectin amounts (10^7 molecules/mm^2) of 5.3 (●), 13 (○), 25 (×), 50 (■), and 310 (□). *Error bars* represent the S.E. from two independent experiments. *C,* ERK2 activation was mediated specifically by fibronectin because a PL-coated surface fails to activate ERK2. Cells were plated on a surface coated with either 0.5 μg/ml Fn or 5 μg/ml PL. After 10 min, cells were lysed, and levels of dually phosphorylated ERK1/2 in 15 μg of whole cell lysate were determined by Western blot. Total ERK1/2 levels were the same for both cases as verified by stripping the blot and reprobing with pan-ERK antibody.

were achieved by an increase in not only ligand density but also integrin expression. Normalizing the initial rate to integrin expression collapses the rate data for the two integrin expression levels onto a single curve, indicating that the initial rate of ERK2 activation is directly proportional to integrin amount (Fig. 4). At low Fn density, this normalized rate was also proportional to Fn amount as shown by a linear curve fit, revealing that the rate of ERK2 activation is simply proportional to the product of the Fn and integrin amount. At high Fn density, the initial rate of ERK2 activation saturated but was still proportional to integrin amount. This shows that the intracellular activation steps performed at a higher rate when more integrin was provided for binding to Fn.

Regardless of the peak level attained, $\alpha_5\beta_1$ integrin-mediated ERK2 activation decays to a basal level by 20 min (Fig. 3, *A* and *B*). This suggests that the rate of ERK2 desensitization is proportional to ERK2 activity, which was confirmed by fitting an exponential decay curve to this portion of the ERK2 activity time course. Calculated decay constants for each Fn coating density and integrin expression level fluctuated around a mean value of 0.3 (± 0.08) min^{-1} and showed no significant dependence on integrin-ligand binding properties (Table I).

Excess Intracellular Machinery Permits Increased Overall ERK2 Response for Increased Integrin Expression Levels—The integral of the ERK2 time course was calculated as a single measure capable of representing both the magnitude and duration of the transient ERK2 signaling response. This integrated ERK2 activity was plotted as a function of Fn coating density for both integrin expression levels (Fig. 5*A*). For a given integrin amount, the integrated ERK2 response increased with increasing Fn coating density, but saturated at high levels of Fn. This saturation was caused by a limitation in integrin-ligand binding because even at these higher saturating Fn densities, allowing more integrin-ligand bond formation by increasing integrin expression caused an increase in the integrated ERK2 response. In fact, when the integrated ERK2 response was normalized to integrin expression level, the normalized values for the 1× and 1.7× integrin expression levels were equal at every Fn coating density, indicating that the overall ERK2 response was directly proportional to integrin expression level (Fig. 5*B*). This direct proportionality indicates that when the binding limitations were relaxed by an increase in integrin amount, the intracellular signaling machinery was sufficiently in excess to promote a proportionally higher ERK2 signal.

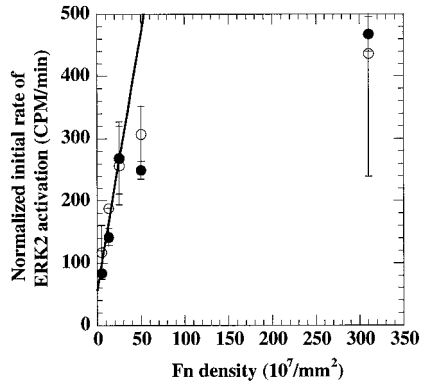

FIG. 4. **The initial rate of ERK2 activation depends on integrin-ligand binding properties.** For each integrin expression level and fibronectin amount, the initial rate of ERK2 was calculated as the slope of the ERK2 activity time course between the 0- and 5-min time points. At each Fn density, this initial rate normalized to the integrin expression level was the same value for the 1× (●) and 1.7× (○) integrin levels, indicating that the initial rate was proportional to integrin expression level. For the lower levels of ligand, a linear curve fit showed that the normalized rate was also proportional to fibronectin density (r^2 = 0.94).

Initial Rates of Signaling via FAK and ERK2 Share Similar Dependence on Integrin-Ligand Binding Properties—To see whether other integrin-mediated signals show similar dependence on integrin-ligand binding, FAK phosphorylation was measured as a function of time (Fig. 6*A*). The time course of FAK phosphorylation significantly differed from the transient pulse response observed for ERK2. Upon exposure to a Fn-coated surface, FAK phosphorylation levels increased for the first 60 min, after which the response reached a suprabasal steady-state level that was maintained for up to 3 h. Similar to the ERK2 response, this FAK response required cell adhesion to Fn as PL failed to induce significant FAK phosphorylation above basal levels (Fig. 6*B*).

Despite the disparate contours of the FAK phosphorylation and ERK2 activity time courses, the two signals were found to have a similar dependence on integrin-ligand binding properties, as revealed by analysis of the initial rates of FAK phosphorylation. The initial rate of FAK phosphorylation was captured by a single measure of FAK phosphorylation level at an early time point (7.5 min), during which it was still increasing in a linear fashion. For both integrin expression levels, the

TABLE I
ERK2 deactivation is a first-order process with respect to ERK2 activity level

For each integrin expression level and fibronectin coating density, the desensitization portion of the ERK2 activity time-course (time points 10, 15, and 20 min) was fit to an exponential decay, and the obtained r^2 values ranged from 0.94 to 0.99. The decay constant fluctuated around a mean value of 0.30 ($\pm$0.08) min^{-1}. Values in parentheses indicate the S.E. of the fit for the decay constant.

$\alpha_5\beta_1$ integrin expression	Fibronectin density	Decay constant
	$10^7/mm^2$	min^{-1}
1×	5	0.20 (0.07)
	13	0.17 (0.02)
	25	0.39 (0.1)
	50	0.26 (0.01)
	310	0.39 (0.06)
1.7×	5	0.25 (0.03)
	13	0.31 (0.11)
	25	0.38 (0.07)
	50	0.31 (0.06)
	310	0.37 (0.17)
Average value		0.30 (0.08)

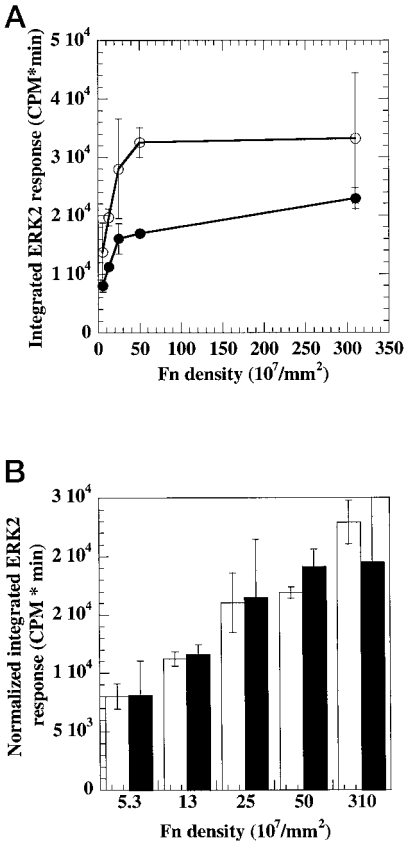

FIG. 5. **The integrated ERK2 response saturated at higher ligand density but increased when integrin expression was raised.** *A,* the integral of the ERK2 time course from 0 to 20 min was calculated for the 1× (●) and 1.7× (○) integrin expression level using the trapezoidal rule: Integrated ERK2 response = (5 min) · (average(E_0, E_5) + average(E_5, E_{10}) + average(E_{10}, E_{15}) + average(E_{15}+ E_{20})), where E_i is the ERK2 activity level at time i for i = 0, 5, 10, 15, and 20 min. *B,* the integrated ERK2 response, when normalized to the integrin expression level, was equal for the 1× (*open columns*) and 1.7× (*filled columns*) integrin expression levels at each fibronectin coating density. This indicates that the overall ERK2 response was proportional to integrin amount. *Error bars* represent the standard error for two independent experiments.

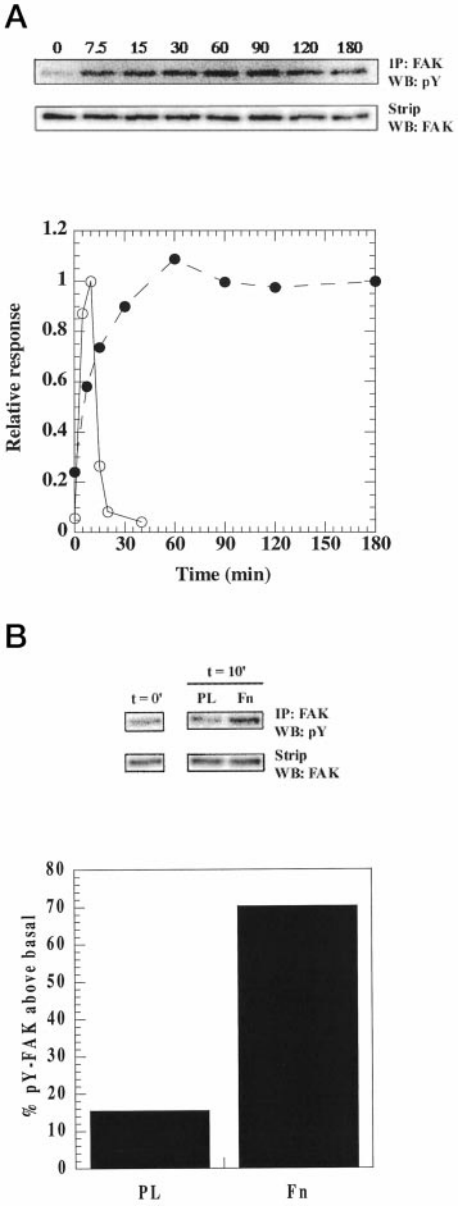

FIG. 6. **The time course of integrin-mediated FAK tyrosine phosphorylation differs from the ERK2 signaling response.** *A,* FAK phosphorylation increases to a nonbasal, steady-state value within 60 min after plating cells on a Fn-coated surface. 1× $\alpha_5\beta_1$ expressing CHO cells were plated on a surface with a Fn density of 50 × 10^7/mm^2. After indicated times, cells were lysed, and immunoprecipitated (*IP*) FAK was analyzed for phosphotyrosine content by Western blot (*WB*). Phosphorylated FAK values were normalized to the total amount of immunoprecipitated FAK, as determined by probing the stripped blot with an anti-FAK antibody. Also depicted for comparison is the ERK2 response upon plating cells on the same Fn density. *B,* cell interaction with fibronectin, but not PL, stimulated significant FAK phosphorylation above the basal level. Cells were plated on a surface coated with either 0.5 μg/ml Fn or 5 μg/ml PL. After 10 min, cells were lysed, and the level of FAK phosphorylation was measured.

initial rate of FAK phosphorylation and ERK2 activation were found to be similar functions of Fn density (Fig. 7). As with ERK2, the initial rate of FAK phosphorylation increased for lower Fn levels and saturated at high Fn surface density, presumably due to limitations in integrin-ligand bond formation.

Proposed Metrics for FAK and ERK2 Signals Correlate to Cell-Substratum Adhesivity—In contrast to requiring the integrated activity as a representative measure of the ERK2 pulse response, the steady-state FAK phosphorylation level can be used to represent the overall FAK response. This steady-state value was measured 90 min after plating cells on a Fn-coated surface. These metrics of the overall FAK and ERK2 signaling response were found to show similar dependence on Fn amount

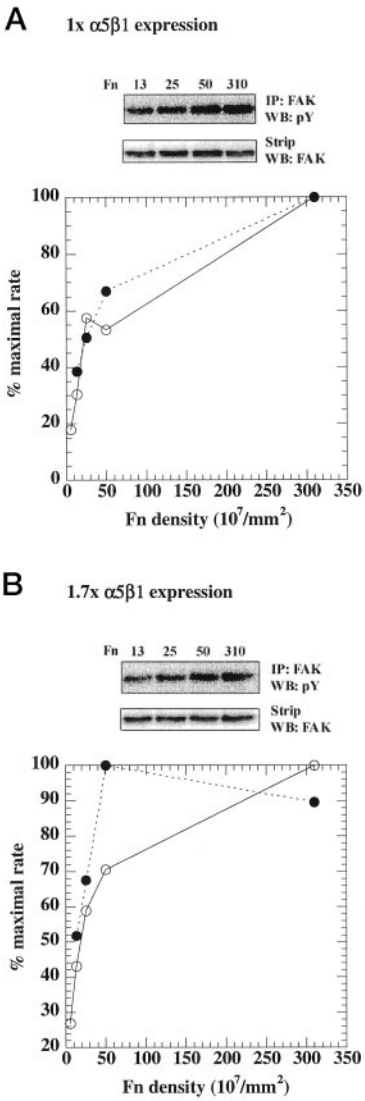

FIG. 7. **Initial rate of ERK2 activation and FAK phosphorylation show a similar dependence on Fn density.** Initial rate of FAK phosphorylation was represented by an early time point (7.5 min) measurement of FAK phosphorylation level by Western blot. The percent maximal rate of ERK2 activation (○) and FAK phosphorylation (●) were determined for 1× (*A*) and 1.7× (*B*) integrin expression levels as a function of Fn amount.

(Fig. 8, *A* and *B*). For low Fn density, an increase in Fn amount resulted in a corresponding increase in both the integrated ERK2 response and the steady-state FAK phosphorylation level. In addition, both these overall responses saturated at similar values of high Fn density.

Similar to signaling, adhesion was specifically mediated by $\alpha_5\beta_1$ integrin-Fn interactions as either soluble RGD (Fig. 8*C*) or anti-human α_5 antibody (data not shown) was able to inhibit cell adhesion to a Fn-coated substratum. This permitted a direct test of whether integrin-Fn binding was the limiting factor for signaling by measuring short term adhesion strength, a value shown to relate to integrin-ligand bond number (24). Due to the sensitivity limit of the centrifugation adhesion assay, adhesive strength given by the mean detachment force was immeasurable for Fn density below $\sim 10 \times 10^7$ molecules/mm^2. Beyond this threshold density, mean detachment force increased initially with increasing Fn density until saturating at higher Fn amount (Fig. 8, *A* and *B*). When the short term cell-substratum adhesivity is compared with the overall FAK and ERK2 signaling responses, it is evident that integrin-ligand bond formation and adhesion directly correlate to the metrics of the FAK and ERK2 signals. In fact, half-maximal mean detachment force, steady-state FAK phosphorylation, and integrated ERK2 activity occurred at similar ligand coating densities in the range of 5–15 $\times$ 10^7 molecules/mm^2. At high ligand density, saturation of FAK and ERK2 signaling corresponds to the saturation of adhesion, confirming that signaling was constrained by integrin-ligand binding limitations.

DISCUSSION

Integrin-mediated signaling involves a complex array of molecules working among synergistic pathways to regulate cell processes. In addition to the complexity of the interconnected biochemical pathways, there may be biophysical constraints on events that are required for maximal signal transduction, such as the aggregation of ligand-occupied integrins and the recruitment of proteins to these aggregated complexes (7, 9). Diffusion or molecular crowding may limit the formation of protein-protein associations and affect activation of downstream components (8). Because the likely complex interplay within this integrated signaling network is not well understood, it is not intuitively apparent how the extracellular integrin-ligand binding event relates to intracellular signaling responses. In this study, we addressed this issue by quantifying FAK and ERK2 signaling in response to manipulating $\alpha_5\beta_1$ integrin interaction with Fn under serum-free conditions, thereby eliminating complicating effects from growth factors and other ECM proteins in serum.

$\alpha_5\beta_1$ integrin interaction with Fn produced a transient biphasic ERK2 response with time, regardless of integrin and Fn amount (Fig. 3, *A* and *B*). This biphasic response results from a balance between pathways that activate and deactivate ERK2. To better understand the positive and negative mechanisms regulating ERK2, we divided our analysis of the signal into two parts. First, to gather insight into the activation mechanisms, the focus was placed on the early part of the response before negative regulation of the signal becomes significant. At these early times, the rate of activation evidently outweighed that of deactivation and ERK2 activity was observed to increase. Several proteins, including p130Cas, Crk, FAK, paxillin, Rho, and Shc, have been identified in pathways leading to integrin-mediated ERK2 activation (3, 5, 7, 15). Furthermore, because Fn possesses other signal-generating domains, such as the heparin-binding domain (31), integrin binding to Fn may initiate an ERK2 response by exposing cryptic sites on Fn that interact with a secondary receptor that directly activates ERK2. Despite the complex involvement of several pathways and molecules leading to ERK2 activation, the observed rate of increase in ERK2 activity was simply proportional to both integrin and Fn levels at low Fn density (Fig. 4).

The simplicity of this dependence gives insight into the cumulative performance of these activation pathways. During the period of initial cell-surface contact, it can be assumed that the number of free integrins is much greater than the number of integrin-Fn complexes and can be treated as a constant with a value approximately equal to the total number of integrins on the cell surface. This assumption also implies that the rate of bond dissociation is relatively small compared with the rate of bond formation. In this case, the number of integrin-Fn bonds would be proportional to the product of the integrin and Fn amounts. Because the rate of increase in ERK2 activity was also a linear function of this product, the initial rate of ERK2 activation seems to be proportional to the number of integrin-ligand complexes at low ligand density. At high ligand density, the rate of increase in ERK2 activity saturates. However, even in this regime, the rate increases when integrin amount is increased, suggesting that ERK2 activation is limited by inte-

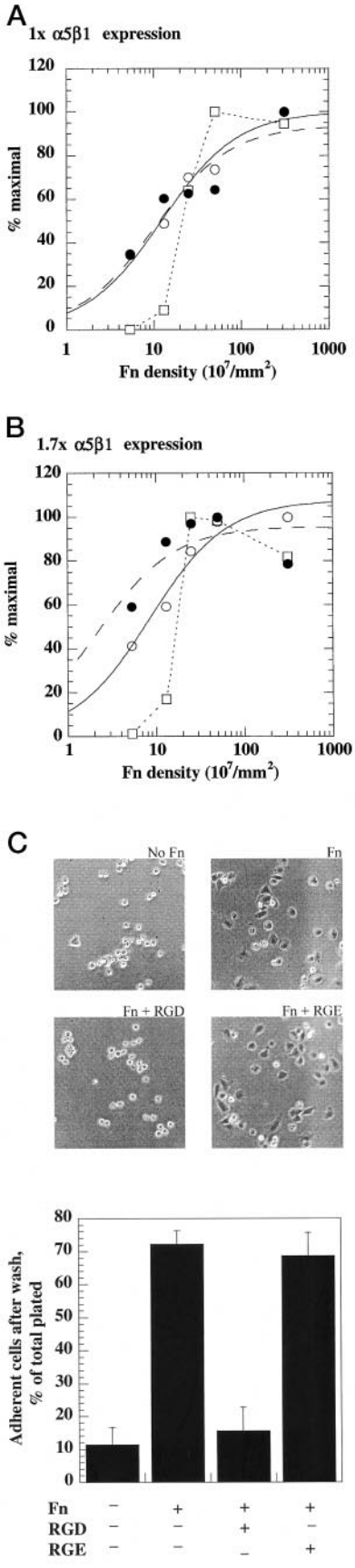

FIG. 8. **Integrin-mediated signaling via ERK2 and FAK correlate with short term cell-substratum adhesivity.** The integrated ERK2 response (○) and steady-state FAK phosphorylation (●) correlate with short term cell-substratum adhesivity (□). CHO cells with 1× (*A*) and 1.7× (*B*) relative expression levels of $\alpha_5\beta_1$ integrin were plated on fibronectin-coated surfaces. The overall ERK2 response was calculated as the integral of the ERK2 time course. Steady-state FAK phosphorylation levels were measured 90 min after plating cells. For short term adhesion measurements, a centrifugation detachment assay was performed. The integrated ERK2 response (——) and steady-state FAK phosphorylation levels (– – – –) were fit to a saturation curve as a function of Fn amount. *C,* cell adhesion required integrin-fibronectin interaction because the absence of Fn or the presence of soluble RGD peptide was able to block adhesion and spreading. 1× $\alpha_5\beta_1$ integrin-expressing CHO cells were plated in microtiter wells either with or without 25×10^7 molecules/mm^2 Fn coating. Those wells that were coated with Fn were also supplied with 1 mM soluble RGD, 1 mM soluble RGE, or no peptide. After 1 h, pictures were taken of a representative view using a phase-contrast microscope. The brightness and contrast of the scanned images were enhanced using Adobe Photoshop. After the 1-h incubation, a wash assay was performed to quantify adhesion. Results are expressed as a percentage of the total number of cells plated.

grin expression and not by intracellular signaling processes.

In the second deactivation-dominated phase, two types of negative feedback mechanisms may be responsible for the observed decay in ERK2 signal. The first involves proteins that catalyze the direct deactivation of ERK2 by dephosphorylation of its tyrosine and threonine residues, including dual specificity phosphatases, such as MKP-1, MKP-2, MKP-3, and PAC-1 (32). Although this phosphatase-mediated deactivation is essential to reduce ERK2 activity levels, these phosphatases would have to function at a rate high enough to surpass the growing impetus for ERK2 activation, as the cells continue to spread and form new integrin-ligand bonds even during the ERK2 signal decay phase. To reduce the load on these phosphatases, a second set of feedback mechanisms may disconnect the sequence of pathways that link the integrin-ligand binding event to the ERK2 signal, thereby countering further ERK2 activation by newly formed integrin-ligand bonds. Several such decoupling mechanisms have been reported that target a number of components upstream of ERK2, including serine/threonine phosphorylation of a proline-rich carboxyl-terminal domain of Sos, hyperphosphorylation of Raf, and phosphorylation on two threonine residues of MEK (33–36).

Instead of focusing on the details of each potential feedback pathway, our aim was to gain quantitative insight into the overall performance of these feedback mechanisms. An interesting result from our quantitative measurements was that regardless of the magnitude of the ERK2 signal, the desensitization was achieved within the same amount of time. Thus, a higher magnitude of ERK2 signal was countered by a proportionally higher magnitude of desensitization in order to reduce the signal in the same time span, a feature indicative of a first-order decay process. An exponential curve fit to the decay portion of the ERK2 time course revealed that the rate of decay was proportional to the ERK2 activity level with a decay constant of 0.3 (± 0.08) min^{-1} (Table I). Therefore, without detailed knowledge of the combination of direct deactivation and/or decoupling events leading to ERK2 signal decay in this system, these feedback processes were shown to perform collectively at a rate determined by the level of active ERK2.

Because ERK2 activation has been shown to be both dependent and independent of FAK in various studies (15–19), the kinetics of FAK phosphorylation was analyzed in order to ascertain the role of FAK as an upstream regulator of ERK2 activity in our system. In contrast to the ERK2 pulse-like response, FAK phosphorylation increased to a suprabasal steady state level after 60 min of stimulation on a Fn-coated surface (Fig. 6*A*). Perhaps surprisingly, the initial increase of ERK2 activity is faster than that of FAK phosphorylation. Furthermore, there was no apparent time lag between the phosphorylation of FAK and the activation of ERK2, as would be expected if FAK phosphorylation were upstream of ERK2

activation. But the absence of this time lag could be attributed to insufficient time resolution of the very early data. Nevertheless, these two observations raise the possibility that FAK-independent pathway(s) may lead to ERK2 activation. However, it can also be argued that ~20% of maximal FAK phosphorylation is present even at time zero, and this may be sufficiently beyond a threshold level of FAK phosphorylation required to stimulate ERK2. Kinetic arguments such as these can be strengthened if the absolute levels, instead of relative values, of phosphorylated FAK and ERK2 activity can be measured. Then, questions such as whether there is a sufficient number of phosphorylated FAK molecules to generate an observed number of active ERK2 molecules can be addressed and thereby shed insight into both the pathway mechanisms and the stoichiometry of the components in these pathways.

Although our data may bring into question whether FAK phosphorylation definitively lies upstream of ERK2 activation or whether these two signaling events lie in parallel pathways, it is apparent from controls (Figs. 3*C* and 6*B*) that these two signals are initiated by a common integrin-ligand binding event and not by adhesion to PL-coated surfaces. However, the apparent disparity in the FAK and ERK2 time courses is not intuitively consistent with the fact that both these signaling responses share the same integrin-Fn binding stimulus. Because later desensitization effects can cloud the link between the stimulus and intracellular signal, we first focused on the early portion of the FAK and ERK2 signals. The initial rates of FAK phosphorylation and ERK2 activation showed a similar dependence on integrin-ligand binding properties (Fig. 7), indicative of their shared stimulus. Therefore, it is likely that the two signaling time courses diverge due to differential regulation of desensitization of FAK phosphorylation *versus* ERK2 activation. Net integrin-ligand bond formation persists as the cells continue to spread until reaching final morphology near 60 min after plating (visual observations, data not shown). Whereas FAK phosphorylation could be coincident with cell spreading and integrin-ligand bond formation, ERK2 activity, as discussed previously, decays from its peak at 10 min to basal levels by 20 min. This suggests that the pathways connecting integrin-ligand bond formation to FAK phosphorylation are not disconnected by feedback pathways, whereas those linking integrins to ERK2 activation are rapidly decoupled.

These kinetic analyses of different portions of the FAK and ERK2 signal lend insight into the activation and desensitization mechanisms but cannot immediately identify the "information content" of a signal. That is, what characteristic measure of the signal is representative of the information carried by that signal to affect downstream cell functions? Consider first the transient ERK2 pulse response and what aspect of this signal can be used to represent the entire signal (Fig. 3, *A* and *B*). Its activity at a single time point is not a suitable representation of the entire response, because both the magnitude and kinetics are affected by changes in integrin-ligand binding properties. For example, choosing one particular early time point, such as 5 min, would underestimate the signal because the peak activity had not yet occurred. Picking a time point associated with the peak level is not a feasible option because the time at which this peak occurred shifts in response to changes in integrin expression and Fn density. Choosing a late time point, such as 20 or 40 min, to measure steady-state ERK2 activity level would lead to the erroneous conclusion that there is no ERK2 response to plating cells on Fn. Furthermore, in physiological terms, the ERK2 activity level at a single time point during a transient response has little significance, because it is possible that ERK2 affects its downstream components each minute that it is active. Therefore, we proposed the integral of the ERK2 activity level as the measure of the overall signaling response for a transient pulse-like signal, because it accounts for the duration of the signal in addition to its magnitude. Furthermore, this integrated amount of activity accounts for shifts in kinetics because the entire time course is used to calculate this value. In contrast, a different approach seems appropriate for signals, such as FAK, phosphorylation that maintain a nonbasal steady-state level. Here, one can argue that the physiologically relevant measure would be its steady-state phosphorylation level, because the phosphorylated signaling molecule has the potential to scaffold with its downstream components as long as it remains phosphorylated.

These two measures were applied to encapsulate the overall FAK and ERK2 signal, and these overall measures were found to correlate with cell adhesion (Fig. 8). For each integrin expression level, the integrated ERK2 response and the steady-state FAK phosphorylation level were increasing monotonic functions of Fn density that saturated at high Fn amount. This saturation paralleled the saturation of short term adhesion, indicating that integrin-ligand binding was the limiting factor in signaling via FAK and ERK2. Even at saturated levels at high ligand density, an increase in integrin expression produced a proportional increase in ERK2 signal, revealing that the intracellular machinery responsible for the ERK2 response is sufficiently in excess to generate more signal once this binding limitation was released by increasing the integrin expression level.

This type of quantitative analysis to other systems can be used to identify bottlenecks in signaling pathways. These limiting factors or events could be powerful disease therapy targets, as relieving or further constricting these bottlenecks would be the most efficient way to enhance or diminish information transfer to a downstream signal. Furthermore, we have implemented an approach of dissecting dynamic signals into their early and late segments to determine the quantitative characteristics of the activation and deactivation mechanisms, which would remain elusive to cursory inspection of disparate time courses. Finally, the rapidly growing interest in signaling ultimately stems from a need to relate these signals to downstream cell processes. To do this, we must identify appropriate metrics of a signal that best correlate to cell behavior, because this would define what aspect of a signal needs to be manipulated to affect downstream cell responses. For such a task, we propose here approaches for two distinct signaling responses. For a pulse-like ERK2 response, a first-time approach of using the integral of its activity was effective in capturing both the duration and magnitude of the signal. On the other hand, for signals such as FAK, the steady-state value may be a valid representation of the signal, because this active/phosphorylated level would be available to continuously work on its downstream target. Future work will focus on whether these proposed or other single-value metrics for encapsulating a dynamic signal generated by both integrins and growth factors can adequately correlate to downstream cell functions and thus be used as parameters in predictive models relating signaling and cell behavior. Such models may provide a rational basis for the design of biomimetic surfaces that specifically activate desired integrin signals or for the determination of target signaling molecules for disease therapies.

Acknowledgments—We thank Jason Haugh and David Schaffer for useful discussions.

REFERENCES

1. Hynes, R. O. (1992) *Cell* **69,** 11–25
2. Lauffenburger, D. A., and Horwitz, A. F. (1996) *Cell* **84,** 359–369
3. Clark, E. A., and Brugge, J. S. (1995) *Science* **268,** 233–239
4. Horwitz, A. F. (1997) *Sci. Am.* **276,** 68–75
5. Schwartz, M. A., Schaller, M. D., and Ginsberg, M. H. (1995) *Annu. Rev. Cell Dev. Biol.* **11,** 549–599

6. Varner, J. A., and Cheresh, D. A. (1996) *Curr. Opin. Cell Biol.* **8,** 724–730
7. Burridge, K., and Chrzanowska-Wodnicka, M. (1996) *Annu. Rev. Cell Dev. Biol.* **12,** 463–519
8. Bray, D. (1998) *Annu. Rev. Biophys. Biomol. Struct.* **27,** 59–75
9. Miyamoto, S., Teramoto, H., Coso, O. A., Gutkind, J. S., Burbelo, P. D., Akiyama, Y., and Yamada, K. M. (1995) *J. Cell Biol.* **131,** 791–805
10. Guan, J.-L. (1997) *Matrix Biol.* **16,** 195–200
11. Klemke, R. L., Cai, S., Giannini, A. L., Gallagher, P. J., de Lanerolle, P., and Cheresh, D. A. (1997) *J. Cell Biol.* **137,** 481–492
12. Mainiero, F., Murgia, C., Wary, K. K., Curatola, A. M., Pepe, A., Blumember, M., Westwick, J. K., Der, C. J., and Giancotti, F. G. (1997) *EMBO J.* **16,** 2365–2375
13. Pozzi, A., Wary, K. K., Giancotti, F. G., and Gardner, H. A. (1998) *J. Cell Biol.* **142,** 587–594
14. Sastry, S. K., Lakonishok, M., Wu, S., Truong, T. Q., Huttenlocher, A., Turner, C. E., and Horwitz, A. F. (1999) *J. Cell Biol.* **144,** 1295–1309
15. Giancotti, F. G. (1997) *Curr. Opin. Cell Biol.* **9,** 691–700
16. Lin, T. H., Aplin, A. E., Shen, Y., Chen, Q., Schaller, M., Romer, L., Aukhil, I., and Juliano, R. L. (1997) *J. Cell Biol.* **136,** 1385–1395
17. Schlaepfer, D. D., Hanks, S. K., Hunter, T., and van der Geer, P. (1994) *Nature* **372,** 786–791
18. Schlaepfer, D. D., and Hunter, T. (1996) *Mol. Cell. Biol.* **16,** 5623–5633
19. Wary, K. K., Mariotti, A., Zurzolo, C., and Giancotti, F. G. (1998) *Cell* **94,** 625–634
20. Chen, Q., Kinch, M. S., Lin, T. H., Burridge, K., and Juliano, R. L. (1994) *J. Biol. Chem.* **269,** 26602–26605
21. Zhu, X., and Assoian, R. K. (1995) *Mol. Biol. Cell* **6,** 273–282
22. Schlaepfer, D. D., Jones, K. C., and Hunter, T. (1998) *Mol. Cell. Biol.* **18,** 2571–2585
23. Argraves, W. S., Suzuki, S., Arai, H., Thompson, K., Pierschbacher, M., and Ruoslahti, E. (1987) *J. Cell Biol.* **105,** 1183–1190
24. Palecek, S. P., Loftus, J. C., Ginsberg, M. H., Lauffenburger, D. A., and Horwitz, A. F. (1997) *Nature* **385,** 537–540
25. Asthagiri, A. R., Horwitz, A. F., and Lauffenburger, D. A. (1999) *Anal. Biochem.* **269,** 342–347
26. DiMilla, P. A., Albelda, S. M., and Quinn, J. A. (1992) *J. Colloid Interface Sci.* **153,** 212–225
27. Lin, T. H., Chen, Q., Howe, A., and Juliano, R. L. (1997) *J. Biol. Chem.* **272,** 8849–8852
28. Miyamoto, S., Teramoto, H., Gutkind, J. S., and Yamada, K. M. (1996) *J. Cell Biol.* **135,** 1633–1642
29. Plopper, G. E., McNamee, H. P., Dike, L. E., Bojanowski, K., and Ingber, D. E. (1995) *Mol. Biol. Cell* **6,** 1349–1365
30. Renshaw, M. W., Ren, X.-D., and Schwartz, M. A. (1997) *EMBO J.* **16,** 5592–5599
31. Bloom, L., Ingham, K. C., and Hynes, R. O. (1999) *Mol. Biol. Cell* **10,** 1521–1536
32. Lewis, T. S., Shapiro, P. S., and Ahn, N. G. (1998) *Adv. Cancer Res.* **74,** 49–139
33. Brunet, A., Pages, G., and Poussegur, J. (1994) *FEBS Lett.* **346,** 299–303
34. Buday, L., Warne, P. H., and Downward, J. (1995) *Oncogene* **11,** 1327–1331
35. Langlois, W. J., Sasaoka, T., Saltiel, A. R., and Olefsky, J. M. (1995) *J. Biol. Chem.* **270,** 25320–25323
36. Wartmann, M., Hofer, P., Turowski, P., Saltiel, A. R., and Hynes, N. E. (1997) *J. Biol. Chem.* **272,** 3915–3923